Numerical Analysis of Bulk Superconducting Magnet Magnetized by Pulsed-Field Considering a Partial Difference of Superconducting Characteristics

K. Yokoyama, T. Oka, H. Fujishiro, and K. Noto

***Abstract*—On the pulsed-field magnetization (PFM) of superconducting bulk magnets, a detailed analysis taking into account the difference in superconducting characteristics between a growth sector boundary (GSB) and a growth sector region (GSR) parts of the material was carried out. The current density was defined in each part and a magnetic field induced by the local current was calculated. The entire magnetic field distribution was obtained by adding individual distributions. The experiment with a Sm123 bulk superconductor was performed and it was confirmed that the calculated distribution agreed with the experimental result.**

***Index Terms*—Bulk superconductor, growth sector boundary/region, magnetic field distribution, pulsed-field magnetization.**

I. Introduction

A SUPERCONDUCTING permanent magnet with RE123 ($\mathrm{RE} = \mathrm{Y}$, Sm, Gd, etc) bulk materials is attracting much attention as one of strong magnetic field generators. This magnet is superior to conventional permanent magnets or iron-cored electro- magnets in strength of generated magnetic field, and thus, various industrial applications such as magnetic separation and magnetron spattering are considered [1]–[4]. The magnetizing method of bulk magnets is roughly divided into a field cooling (FC) and a pulsed-field magnetization (PFM). In the former, a high magnetic field can be captured and a magnetic field exceeding 17 T at 29 K is achieved [5]. On the other hand, PFM is an important technique for various industrial applications because a bulk can be magnetized with a simple and relatively cheap apparatus in a short time. However, there is a problem that the strength of trapped field (B_{T}) is less than a half of that magnetized by FC at low temperature below about 50 K. The IMRA (iteratively magnetizing pulsed-field operation with reducing amplitudes) method [6], [7], MPSC (multi pulse technique combined with a stepwise cooling) method [8] and MMPSC (modified MPSC) method [9] are developed recently aiming at improvement of B_{T} in PFM ($B_{\mathrm{T}}^{\mathrm{PFM}}$) and $B_{\mathrm{T}}^{\mathrm{PFM}}$ of over 5 T is achieved by the MMPSC method. These are magnetizing methods in which several pulsed-fields are applied with changing the strength of magnetic fields and cooled down temperature based on the idea of controlling heat generation of the bulk during the magnetization. The heat generation influences a critical current density J_{c}, and thus, the resulted B_{T} also changes [10], [11]. Moreover, it is known that there is a difference in J_{c} characteristics between a growth sector boundary (GSB) and a growth sector region (GSR) parts in the same material, and the characteristics of the former are more excellent than that of the latter [7]. In FC method, the difference between two parts hardly influences the performance of the trapped field because, in this case, heat generation is mostly caused by the flux flow during the decreasing exciting field which is very slow in FC method, and thus the temperature rise is very small. In PFM, on the other hand, heat generation originates mainly from flux jump and it is different locally according to J_{c}.

This paper presents a detailed analysis method taking into the consideration of the difference in the J_{c} characteristics between GSB and GSR parts for the purpose of theoretical clarification of magnetizing mechanism and development of more efficient magnetizing method. Firstly, a Sm123 bulk superconductor is magnetized by PFM with changing the magnitude of applied peak field from 3.10 to 5.42 T. Temperature and trapped field at the bulk surface are monitored during the magnetization, and the trapped field distribution above 3.5 mm from the surface is scanned after the magnetization. Next, a current distribution is estimated from the experimental results and the magnetic field distribution is calculated by using the proposed analysis model and the obtained current distribution. The validity of the simulation method is verified from the agreement between experimental and numerical results.

II. Experiment

A. Bulk Material and Measurement Procedure

Fig. 1 shows a melt-processed Sm123 bulk superconductor used in this experiment. The growth sector boundaries (GSB) that appear in the process of the crystal growth can be clearly seen. The bulk material is a highly c-axis oriented crystal and consists of $\mathrm{SmBa_2Cu_3O_y}$ (Sm123), $\mathrm{Sm_2BaCuO_5}$ (Sm211) with the molar ratio of 1.0:0.3, 0.5 wt.% Pt powder and 1.5 wt% $\mathrm{Ag_2O}$ addition. The size of the sample is 46 mm in diameter and 15 mm in thickness and it is impregnated by epoxy resin reinforced by glass fiber. The epoxy resin on the upper and

Manuscript received August 28, 2007. This work was supported in part by the CREAT IWATE Project driven by the Japan Science and Technology Organization.

K. Yokoyama is with the Department of Electrical and Electronic Engineering, Ashikaga Institute of Technology, 268-1 Omae-cho, Ashikaga, Tochigi 326-8558, Japan (e-mail: k-yokoyama@ashitech.ac.jp).

T. Oka is with Education Center for Engineering and Technology, Faculty of Engineering. Niigata University, 2-8050, Ikarashi, Nishi-ku, Niigata 950-2181, Japan (e-mail: okat@eng.niigata-u.ac.jp).

H. Fujishiro is with the Faculty of Engineering, Iwate University, 4-3-5 Ueda, Morioka 020-8551, Japan (e-mail: fujishiro@iwate-u.ac.jp).

K. Noto is with Iwate University (e-mail: notokoshichi@yahoo.co.jp).

Digital Object Identifier 10.1109/TASC.2008.920530

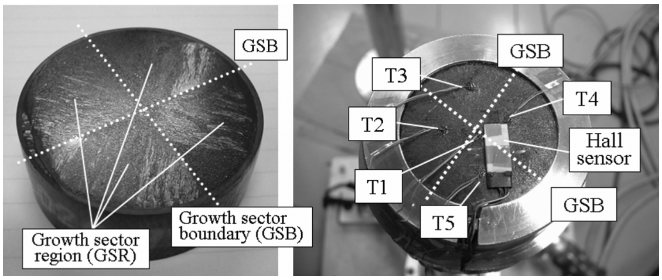

Fig. 1. A melt-processed Sm123 bulk material and set-up for measurement of temperature and trapped field.

lower sides of the bulk was removed in order to establish the thermal contact to the thermocouples and to measure the precise temperature and to reduce a thermal contact resistance to the cold head.

The bulk is set on a copper base connected to a cold head of Gifford-McMahon (GM) cycle refrigerator (AISIN SEIKI CO., LTD, GR301). Five Teflon-coated chromel-constantan thermocouples (T1–T5) of 76 $\mu\mathrm{m}$ in diameter are adhered on the surface of bulk superconductor using the GE7031 varnish. T1 is put on the center of the sample and T2–T5 are arranged in four GSRs as shown in the insets of Fig. 1. A Hall sensor (F.W.Bell, BHT-921) is set near T1 to monitor a magnetic flux density of trapped field as shown also in the insets.

B. Magnetization and Results

A temperature and a trapped field distribution in FC and PFM are measured. In FC magnetization, a static field of 5 T is applied to the bulk material at an initial temperature of 100 K by a solenoid type superconducting magnet with a field of 10 T and a room-temperature-bore of 100 mm in diameter (JASTEC, JMTD-10T100), and afterward the bulk is cooled down to a prescribed temperature (40, 50, 60 and 70 K at the cold stage). After temperature of all thermocouples steady, the magnetic field is reduced to zero with a sweep rate of −5.06 mT/s. A temperature and a magnetic field are measured every 8 seconds. In PFM, the bulk is cooled down to 40 K at the cold stage, and afterward pulsed-field of 3.10, 3.83, 4.64 and 5.42 T with a rising time of 10 ms is applied. A temperature and a magnetic field are monitored about 7 times per second. After each magnetization, the axial components of trapped magnetic flux density above 3.5 mm from the bulk surface are scanned by a Hall sensor (F.W.Bell, BHA-921).

Fig. 2 shows the time response of temperature of T2–T5 for pulsed fields of $\mu_0 H = 3.10$ T and 4.64 T. For the case of $\mu_0 H = 3.10$ T, the temperature at T4 and T5 rise faster and higher than ones at other parts. It means that magnetic flux enters in the bulk only through T4 and T5parts. For the case of $\mu_0 H =$ 4.64 T, on the other hand, the temperature at all the points rise up at the same time. It is considered that magnetic flux enters in the bulk from the whole periphery. When each maximum temperature is compared, it reaches about 70 K for $\mu_0 H = 4.64$ T though it is about 50 K for $\mu_0 H = 3.10$ T. It is because heat generation caused by pinning loss grows with increase in the amplitude of applied pulsed-field.

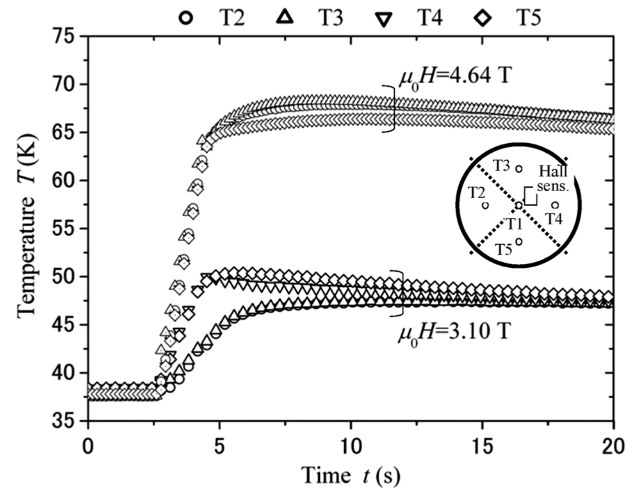

Fig. 2. The time responses of temperature at T2–T5 for the applied pulsed-field $\mu_0 H = 3.10$ T and 4.64 T.

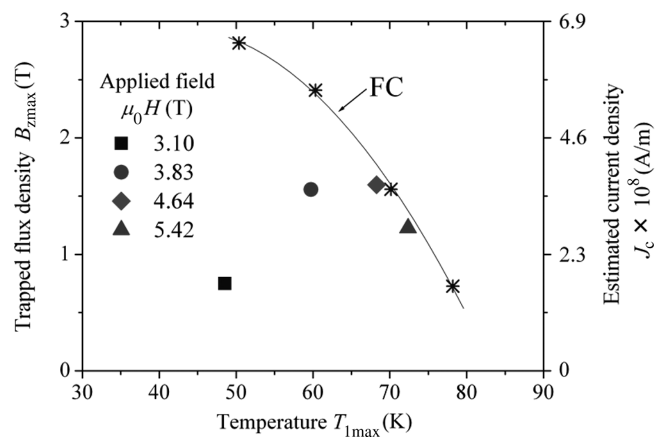

Fig. 3. The temperature dependence of trapped flux density for the various applied pulsed-fields. The horizontal and vertical axes indicate the maximum temperature at T1 and the maximum z-direction flux density in the horizontal plane above 3.5 mm from the bulk surface, respectively. The relationship for the FC magnetization is also presented. A right axis indicates the estimated current density.

Fig. 3 shows the temperature dependence of trapped field. The horizontal and vertical axes indicate the maximum temperature at T1 and the maximum z-direction field measured above 3.5 mm from the bulk surface, respectively. The relationship in FC magnetization is also presented. The temperature increases monotonously with the applied field. On the other hand, the trapped maximum field increases with the applied pulsed field from $\mu_0 H = 3.10$ T to 4.64 T, but, thereafter it decreases along the FC line which indicates the upper limit of trapped field for each temperature. These results suggest that a high applied field causes high temperature rise, and thus, a trapped field is reduced due to the decrease in J_c.

Fig. 4 illustrates the two- and one-dimensional trapped field distributions measured above 3.5 mm from the bulk surface for an applied pulsed-field of (a) $\mu_0 H = 3.10$ T and (b) 4.64 T, respectively. For the reference, the result in FC with a static applied field of 5 T and the bulk temperature of 70 K is presented in Fig. 4(c). One-dimensional distributions show cross sections of two- dimensional maps cut by GSR1, GSR2, GSB1

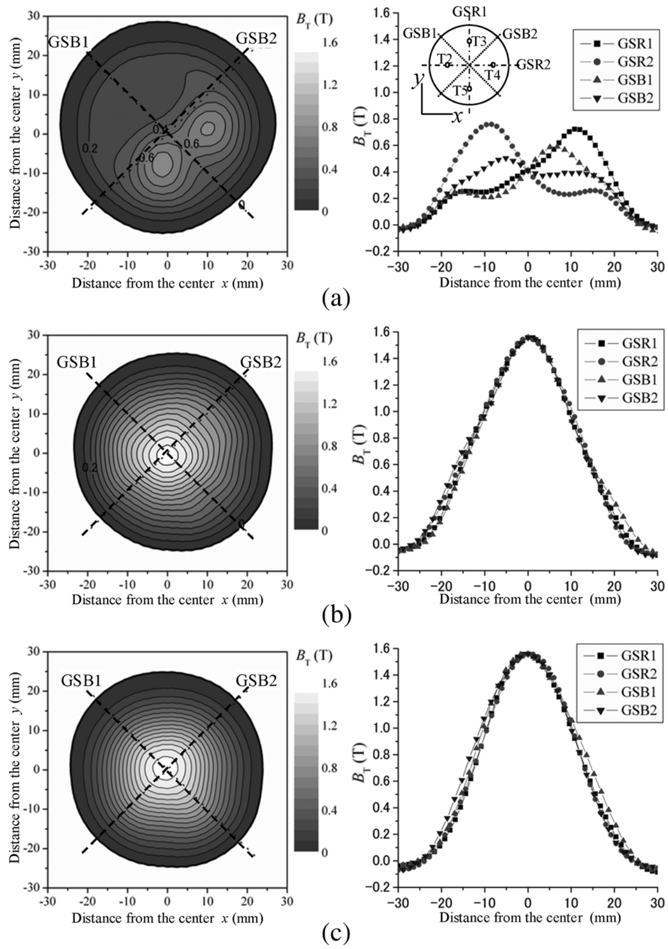

Fig. 4. Two- and one-dimensional distributions of trapped magnetic field. Two-dimensional maps are measured in the horizontal plane above 3.5 mm from the bulk surface in PFM of (a) $\mu_0 H = 3.10$ T and (b) 4.64 T, and (c) FC with the applied static field of 5 T and the bulk temperature of 70 K. One-dimensional maps show cross sections of two-dimensional maps cut by GSR1, GSR2, GSB1 and GSB2 lines indicated in (a). (Experimental results).

and GSB2 lines indicated in Fig. 4(a). For the case of $\mu_0 H = 3.10$ T, there are two peaks at T4 and T5 parts with the maximum magnetic flux densities of 0.72 T and 0.76 T, respectively. The same experiment was carried out several times and it was confirmed that the magnetic flux was always trapped only at the same parts. From this result, it is estimated that J_c characteristics at T4 and T5 parts are low compared with other parts. For the case of $\mu_0 H = 4.64$ T, the distribution almost agrees with one for FC with a static applied field of 5 T and the bulk temperature of 70 K. This is corresponding to the result that the points of PFM of $\mu_0 H = 4.64$ T and FC at 70 K almost overlap as shown in Fig. 3. Although both draw a concentric circle with a peak value of 1.56 T, one can see that a lot of magnetic flux is trapped at GSR part in PFM, but the relationship is opposite in FC. Because there is little influence of flux creep by heat generation in FC and the J_c characteristic is directly reflected in the magnetic field distribution, it is understood that J_c in GSB is higher than one in GSR. In PFM of $\mu_0 H = 4.64$ T, on the other hand, it is thought that the strength of applied field is not enough for the magnetic flux to be trapped in the GSB parts.

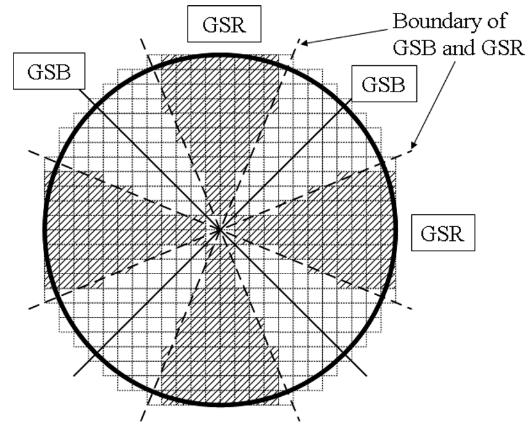

Fig. 5. Simulation model of the bulk magnet. The sample is evenly divided into eight regions, each four regions of GSB and GSR.

III. Numerical Analysis

A. Simulation Model

A numerical analysis of PFM is carried out on the basis of the experimental results. Although the final aim is to imitate the movement of magnetic flux during the magnetization, the dynamic pinning characteristics are not considered and they are evaluated as distribution of J_c after the magnetization in this paper.

Fig. 5 shows a simulation model of the bulk magnet. The sample is evenly divided into eight regions, each four regions of GSB and GSR, and it is assumed that the area of each part is equal for convenience. The current densities in GSB and GSR parts are defined as J^{GSB} and J^{GSR}, respectively, assuming that ones in four regions of each part are equal. These values are calculated from the slope of the one-dimensional distributions of trapped field shown in Fig. 4 in accordance with the Bean model, though a bulk superconductor is not necessarily a critical state. By using estimated current density and the proposed simulation model, the magnetic field induced by J^{GSB} and J^{GSR} is calculated by the following expression.

$$\left.\begin{aligned} \boldsymbol{B} &= \mathrm{rot}\boldsymbol{A} \\ \nabla^2 \boldsymbol{A} &= \mu_0 \boldsymbol{J} \end{aligned}\right\}, \tag{1}$$

where $\boldsymbol{A}$ and μ_0 are the vector potential and the magnetic permeability of the vacuum, respectively. The entire magnetic field distribution is obtained by adding individual distributions.

B. Results and Discussion

A critical current J_c corresponding to the maximum flux density of trapped field $B_{\max}$ is calculated from experimental results of FC by (1). The estimated J_c is indicated in the right axis in Fig. 3. In the case of FC, J^{GSB} is almost equal to J_c and $J^{\mathrm{GSB}} = 3.59 \times 10^8$ A/m^2. Also, J^{GSR} is 2.2% smaller than J^{GSB}. In the case of PFM of $\mu_0 H = 4.64$ T, J^{GSB} and J^{GSR} are 2.72×10^8 A/m^2 and 3.26×10^8 A/m^2, respectively, and J^{GSR} is 16.9% larger. In the case of $\mu_0 H = 3.10$ T, $J^{\mathrm{GSR}} = 2.05 \times 10^8$ A/m^2 and $J^{\mathrm{GSB}} = 0.87 \times 10^8$ A/m^2, and J^{GSB} is below the half of J^{GSR}.

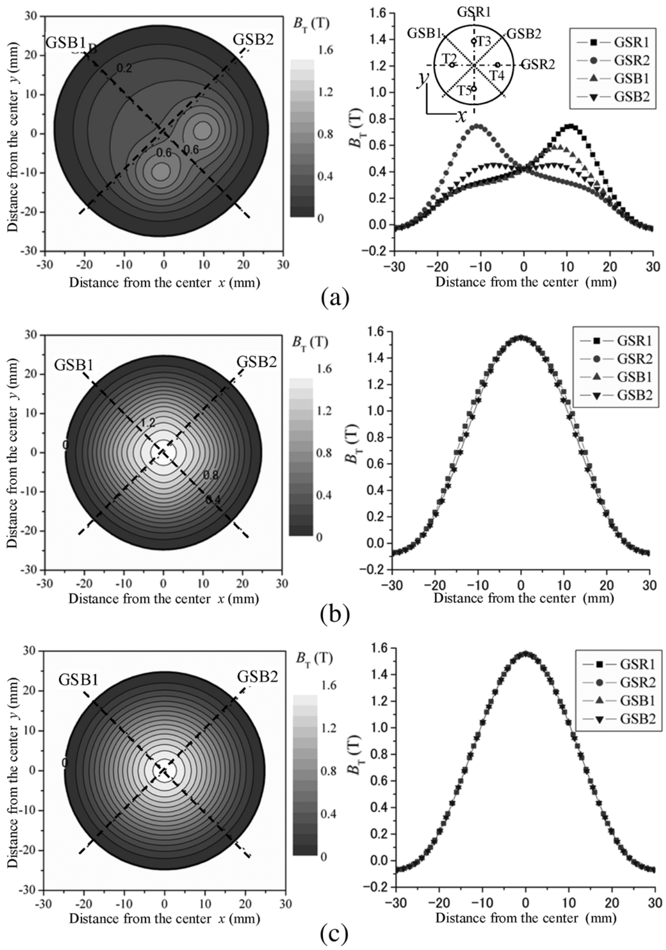

Fig. 6. Two- and one-dimensional distributions of trapped magnetic field. Two-dimensional maps are measured in the horizontal plane above 3.5 mm from the bulk surface in PFM of (a) $\mu_0 H = 3.10$ T and (b) 4.64 T. A result by the ordinary method in PFM of $\mu_0 H = 4.64$ T is presented in (c). One-dimensional maps show cross sections of two- dimensional maps cut by GSR1, GSR2, GSB1 and GSB2 lines indicated in (a). (Numerical results).

A magnetic field distribution is calculated by using a simulation model shown in Fig. 5 and the above J^{GSB} and J^{GSR} values. Fig. 6 shows the simulation results of two- and one-dimensional distributions of magnetic field for PFM of (a) $\mu_0 H =$ 3.10 T and (b) 4.64 T. A result by an ordinary model in which the difference between J^{GSB} and J^{GSR} is not considered is also presented in Fig. 6(c) for the reference. In Fig. 6(a), the current loops in T2 and T3 parts are deleted according to the experiment result. Though the estimation of J^{GSB} is difficult, the agreement between the numerical and experimental results is obtained. In Fig. 6(b), a local characteristic at GSB parts is appeared while the result by the ordinary model is a complete concentric circle shown in Fig. 6(c). Moreover, a good correspondence to the experimental result is shown. As mentioned above, the experimental results are reproduced well by this analysis, and the validity of the proposed method is confirmed.

IV. Conclusions

A bulk superconductor magnetized by PFM was analyzed in detail by using a simulation model taking into account the difference in the J_c characteristic between GSB and GSR parts. Firstly, the experiment of PFM with a Sm123 material was performed. A temperature and magnetic flux density at the bulk surface were measured during the magnetization and a trapped field distribution above 3.5 mm from the surface was scanned. For a low applied field of 3.10 T, magnetic flux was trapped only in GSR parts. For a high applied field of 4.64 T, the distribution drew a concentric circle as well as the result in FC, but the trapped magnetic flux in GSR parts was more than that in GSB parts. Next, current densities in GSB and GSR parts were estimated from experimental results, and magnetic distributions were calculated by using the obtained values and the simulation model. The numerical results agreed with the experimental ones, and thus, it was confirmed to be able to analyze the current distribution in detail by the proposed method. We will carry out the magnetizing simulation considering magnetic flux motion during the magnetization.

References

[1] N. Saho, H. Isogami, T. Takagi, and M. Morita, "Continuous superconducting -magnet filteration system," *IEEE Trans. Appl. Supercond.*, vol. 9, no. 2, pp. 398–401, Jun. 1999, accepted for publication.

[2] Y. Yanagi, T. Matsuda, H. Hazama, K. Yokouchi, M. Yoshikawa, Y. Itoh, T. Oka, H. Ikuta, and U. Mizutani, "Generation of strong magnetic field using 60 ϕ superconducting bulk magnet and its application to magnetron sputtering device," *Physica C*, vol. 426–431, no. 1, pp. 764–769, Oct. 2005.

[3] N. Koshizuka, K. Matsunaga, N. Yamachi, A. Kawaji, H. Hirabayashi, M. Murakami, M. Tomita, S. Une, S. Saito, M. Isono, H. Nasu, T. Maeda, and F. Ishikawa, "Construction of the stator installed in the superconducting magnetic bearing for a 10 kWh flywheel," *Physica C*, vol. 412–414, no. 1, pp. 756–760, Oct. 2004.

[4] K. Yokoyama, T. Oka, H. Okada, Y. Fujine, A. Chiba, and K. Noto, "Solid-liquid magnetic separation using bulk superconducting magnets," *IEEE. Trans. Appl. Supercond.*, vol. 13, no. 2, pp. 1592–1595, Jun. 2002.

[5] M. Tomita and M. Murakami, "High temperature superconductor bulk magnets that can trap magnetic fields of over 17 tesla at 29 K," *Nature*, vol. 421, no. 6922, pp. 517–520, Feb. 2003.

[6] U. Mizutani, T. Oka, Y. Itoh, Y. Yanagi, M. Yoshikawa, and H. Ikuta, "Pulsed-field magnetization applied to high- T_c superconductors," *Appl. Supercond.*, vol. 6, no. 2–5, pp. 235–246, Feb. 1998.

[7] H. Ikuta, T. Hosokawa, H. Ishihara, M. Yoshikawa, Y. Yanagi, Y. Itoh, T. Oka, and U. Mizutani, "Melt-processed RE-Ba-Cu-O ($\mathrm{RE} = \mathrm{Sm}$, Nd) superconductors for quasi-permanent magnets," *IEEE Trans. Appl. Supercond.*, vol. 11, no. 1, pp. 3716–3719, Mar. 2001.

[8] M. Sander, U. Shutter, R. Koch, and M. Läser, "Pulsed magnetization of HTS bulk parts at $\mathrm{T} < 77\ \mathrm{K}$," *Supercond. Sci.,Technol.*, vol. 13, no. 6, pp. 841–845, Jun. 2000.

[9] H. Fujishiro, T. Tateiwa, A. Fujiwara, T. Oka, and H. Hayashi, "Higher trapped field over 5 T on HTSC bulk by modified pulse field magnetizing," *Physica C*, vol. 445–448, no. 1, Oct. 2006.

[10] H. Fujishiro, T. Oka, K. Yokoyama, and K. Noto, "Time evolution and spatial distribution of temperature in YBCO bulk superconductor after pulse field magnetizing," *Supercond. Sci. Technol.*, vol. 16, no. 7, pp. 809–814, Jul. 2003.

[11] K. Yokoyama, M. Kaneyama, H. Fujishiro, T. Oka, and K. Noto, "Temperature rise and trapped field in a GdBaCuO bulk superconductor cooled down to 10 K after applying pulsed magnetic field," *Physica C*, vol. 412–414, no. 1, pp. 671–675, Oct. 2005.